Low-dose Thallium-induced neurotoxicity: early-onset mitochondrial dysfunction in living hippocampal neurons and correlation with ethanol production

Emilia Bramanti[1¶], Massimo Onor[1¶], Laura Colombaioni[2*]

[1] National Research Council of Italy, C.N.R., Institute of Chemsitry of Organo Metallic Compounds-ICCOM, Pisa, Italy.

[2] CNR Neuroscience Institute, Area della Ricerca CNR, Pisa, Italy.

Manuscript revised for *ACS Chemical Neuroscience,October 1st* 2018

Abstract

The heavy metal Thallium (Tl) is an emerging pollutant among the most potentially toxic species to which human populations are exposed. Its harmful effects on living organisms are well known at high doses, typical of acute intoxication. Its harmful effects at low doses are by far less known.

In a previous paper we reported a TlCl-induced metabolic shift to lactate and ethanol production in living hippocampal HN9.10e neurons that appeared after a single short exposure (48 h) at low -doses (1-100 μg/L). This metabolic shift to lactate and ethanol suggestes a marked impairment of cell bioenergetics.

In this work we provide detailed evidence for TlCl-induced changes of neuronal morphology and mitochondrial activity. Confocal microscopy and fluorescent probes were used to qualitatively and quantitatively analyze, at sub-cellular level, the living HN9.10e neurons during and after the TlCl exposure. An early-onset mitochondrial dysfunction appeared, associated with signs of cellular deregulation such as neurite shortening, loss of substrate adhesion and increase of cytoplasmic calcium. The dose-dependent alteration of mitochondrial ROS (mtROS) level and of transmembrane mitochondrial potential ($\Delta\Psi_m$) has been observed also for very low TlCl doses (1 μg/L). The treatment with the ATP synthase inhibitor oligomycin revealed a severe impairment of the mitochondrial function, more significant than that measured by the simple quantification of the TMRM fluorescence. These results highlight that mitochondria are a key sub-cellular target of TlCl neurotoxicity .The transmembrane mitochondrial potential was significantly correlated with the ethanol concentration in cell culture medium ($P < 0.001$, $r = -0.817$), suggesting that ethanol could be potentially used as a biomarker of mitochondrial impairment.

Keywords: thallium neurotoxicity; hippocampal neurons; mitochondrial dysfunction; confocal microscopy.

Abbreviations:

i.v. intra venous

SPECT Single Photon Emission Computed Tomography

CNS Centra Nervous System

mtROS (mitochondrial ROS)

$\Delta\Psi_m$ (mitochondrial transmembrane potential)

MT-ROS (MitoTracker™ Red CM-H_2XRos)

Fluo-3AM (Fluo-3 acetoxymethylester)

TMRM (tetramethylrhodamine methyl ester)

EtOH (ethanol)

CCM cell culture medium

INTRODUCTION

Thallium is a rare metal, very toxic for biological systems. Although the nervous system is a very important target of this element, most of the Tl toxicity studies have been focused on non-neuronal tissues such as liver, kidney, muscle and in cardiovascular system.[1-5]. In these tissues serious damages on various sub-cellular organelles have been highlighted, in particular on mitochondria, endoplasmic reticulum and lysosomes.[1-5] Few authors have been reported about the cellular and molecular mechanisms responsible of Tl toxicity and the concentrations explored in these studies were >500 μg/L.[6-9] Despite the great interest of these studies, the concentrations at stake are in fact much higher than the concentrations recently found in drinking water of some contaminated regions.[10, 11] Thus, it is important to explore the Tl toxicity also at lower concentrations. Growing evidence supports the link between the exposure to very low Tl levels and neurotoxicity. However, until now, the environmental rarity of Tl has caused a serious underestimation of its potential risk to human health. Even less data are reported on Tl neurotoxicity and the effects of Tl on the nervous system have been described mainly from a clinical point of view: insomnia, irritability, axonal degeneration, myelin loss, severe central and peripheral neuropathy with ataxia and paralysis are the key neurological symptoms of Tl intoxication.[12-14]

The high-affinity uptake of Tl by human neurons is clearly demonstrated by its use in medical diagnostics as a tracer of brain tumors[15-17] and in brain trauma evaluation.[18] Despite the low doses injected (,30-40 μg i.v. injection in CNS Single Photon Emission Computed Tomography, SPECT, corresponding to about 6-7 μg/L Tl in blood,) the images collection usually starts after only 5-10 min showing the quick entry of TlCl into the neuronal cytoplasm. Moreover its permanence inside neurons lasts more than 24 hours after the injection.[15-18]

Thallium has an analogous behavior when used in myocardial imaging (20 μg 1.v. injection in 70 kg subject) reaching the cytoplasm of cells in few minutes.[19-21] Its permanence in heart cells and other cell types is equally prolonged over the time: up to 24-36 after the injection especially in kidney (13%), bones (11%), gut (25%), heart (5%), testicles (5%) and thyroid (6%).

The lack of in-depth knowledge of the specific molecular mechanisms that lead to neuronal dysfunction prevents the development of effective therapeutic approaches to limit or reverse the neurological damage resulting by contamination with Tl.

Recently we published a study on the consequences on the neuronal metabolism of a short and transient exposure to low TlCl doses.[22] The TlCl exposure increased the production of lactate and ethanol, quantitatively determined in the culture medium, suggesting that the processes involved in neuronal energy production are impaired. Whereas the lactate metabolism is biochemically well characterized and its increase in stress conditions is widely reported,[23-26] the neuronal ethanol (EtOH) production is by far less investigated and never studied in neuronal cells.

McManus et al. described the production of EtOH by human cells for the first time in 1960[27] but after this the production of EtOH by human cells and mammalian tissues (namely *endogenous*)[27] has never been systematically studied and it was only occasionally reported in association with pathological conditions.[28-32]

The cellular mechanisms underlying EtOH production remains a poorly explored phenomenon, As both the lactate and the EtOH production are related to alteration in energy production,[33, 34] we can hypothesize that mitochondria are directly involved in the TlCl-mediated toxicity that has as effect the production of lactate and EtOH.

In this work we investigated living HN9.10e neurons using confocal microscopy and fluorescent probes to qualitatively and quantitatively analyze at sub-cellular level the alterations of mitochondria during and after the Tl exposure. The results herein reported demonstrate that TlCl doses much lower than those considered safe for human environmental exposure induce significant mitochondrial alterations. The possible employment of EtOH as a marker of mitochondrial impairment is discussed.

RESULTS AND DISCUSSION

Tl toxicity on HN9.10e neurons

Thallium is well known for its pronounced toxicity to biological systems. The nervous system is one of the main targets of Tl intoxication. Both neurons (and cells in general) accumulate Tl^+ because of its chemical similarity to K^+, a physiological ion fundamental for the transmission of electrical signals.

Although the neurological symptoms of Tl intoxication are known, the molecular bases of its neuronal toxicity remain poorly characterized.

In a previous study (Colombaioni et al.)[22] we shown that the transient exposure to low TlCl doses (1, 10 and 100 μg/L) induces in the hippocampal neurons HN9.10e metabolic changes that lead to an enhancement of lactate and ethanol production, with a remarkable prevalence of ethanol at the highest, and most toxic TlCl dose (100 μg/L). These TlCl concentrations are much lower than those employed in other Tl toxicological studies[6-9] and are related to the concentrations recently found in drinking water of some contaminated regions.[10, 11]

In this and in the previous work[22] HN9.10e neurons were exposed to TlCl instead of the widely and most used $TlNO_3$ species. We observed, indeed, that NO_3^- ions itself had remarkable effects on several mitochondrial properties such as the aggregation state, the membrane potential ($\Delta\Psi_m$) and ROS production (unpublished result).

The exposure to 10 μg/L TlCl reduced the cell density by the induction mainly of apoptosis (up to 50%) and in lesser extent of necrosis.[22] In cell cultures exposed to 100 μg/L Tl we observed up to 50% cell death, exclusively due to necrosis. We hypothesized that this phenomenon is correlated with a severe metabolic dysfunction that drastically reduces the cellular energy charge, interfering with all the active, energy-dependent cellular processes, including apoptosis, due to a critical impairment of mitochondria and of their capacity of producing energy.[35]

In order to further investigate the mitochondrial function we evaluated immediately 48 h after the exposure and during the recovery in TlCl-free medium (at 24 h, 48 h and 72 h to examine if and how long the effects persisted): (i) the intra mitochondrial ROS level (mtROS), (ii) the

transmembrane potential $\Delta\Psi_m$. We selected the TlCl doses and exposure time previously employed[22] that gave the enhancement of lactate and ethanol concentration level.

The existence of a sub-lethal temporal window, which avoided an immediate, massive cell death, allowed us to study the early neuronal responses, representative of the physiological compensatory reaction to stress.

TlCl alters the cytoplasm texture in transmitted light: it becomes more granular and inhomogeneous and in the case of the exposure to 100 μg/L TlCl vacuoles are formed. Furthermore, TlCl exposure affects the length of the processes emerging from cell bodies and the degree of substrate adhesion.

Figure 1 shows the morphology and the relative frequency distribution of neurite length (μm) of HN9.10e neurons in controls and after 48 h exposure to TlCl.

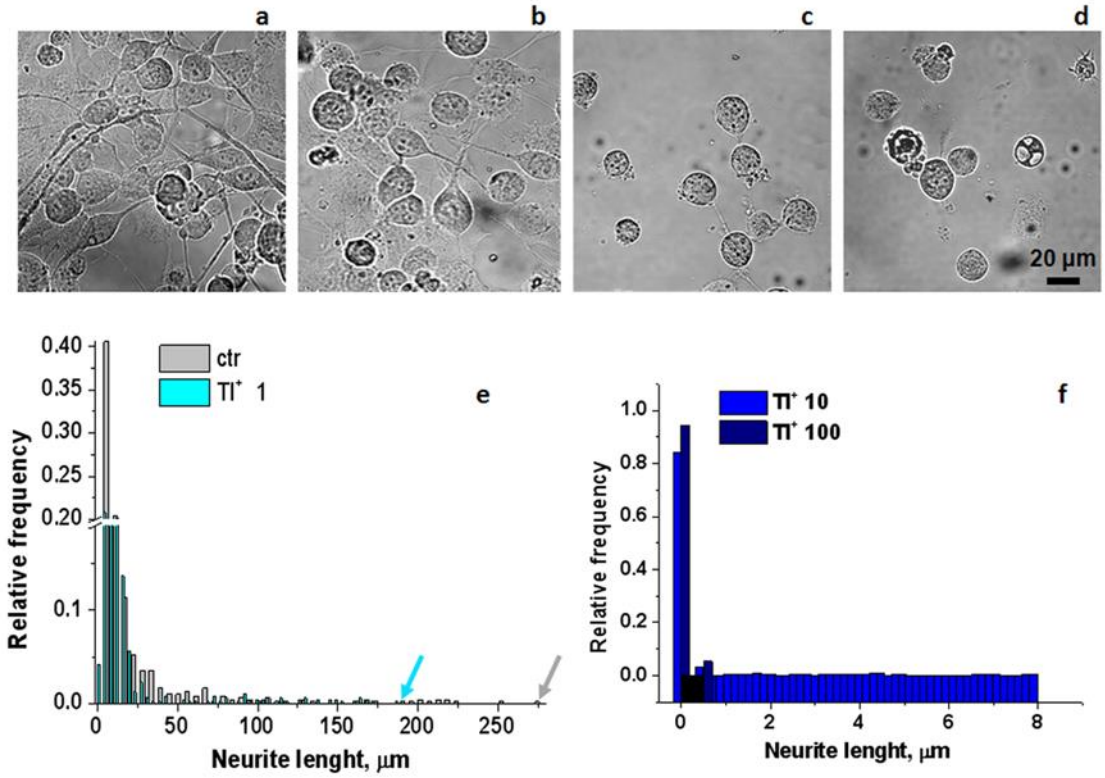

Figure 1. Morphology of HN9.10e neurons in controls (a) and after 48 h exposure to 1 (b), 10 (c) and 100 μg/L TlCl single dose (d). The relative frequency distribution of neurite length (μm) is

reported for control and 1 μg/L TlCl single dose (e panel) and for 10 and 100 μg/L TlCl single dose (f panel).

Table 1 reports the summary statistic of neurite length in control and TlCl treated cultures (Kruskal-Wallis non parametric test).

Table 1. Summary statistic of neurite length in control and TlCl treated cultures (450 images from N =3 independent experiments).

	Minimum length	Maximum length	Mean length	Standard deviation
Ctr	5.9	276.6	24.5	38.5
1 μg/L Tl	2.4	189.0	22.0	33.1
10 μg/L Tl	0	8.0	0.48***	1.4
100 μg/L Tl	0	0.5	0.03***	0.11

Asterisks indicate significant differences (Kruskal-Wallis test) with respect to control cultures (* =P <0.05; ** P<0.01; *** = P<0.001; N =3 independent experiments).

The decrease of the length of neuronal processes was not significant (P > 0.05) after 48 h exposure to 1 μg/L TlCl in terms of average values and it was significant (P< 0.001) after 10 and 100 μg/L Tl. However, the data of Figure 1 (e) show that 1 μg/L TlCl was enough to decrease the length of neuronal processes (2-190 μm range) with respect to control (6-277 μm range). The exposure to 10 and 100 μg/L TlCl gave also a substantial loss of substrate adhesion *vs* the control group.

In agreement with our previous results,[22] we found a significant viability loss for TlCl doses $\geq$ 10 μg/L. At the highest TlCl dose (100 μg/L) cell death was exclusively of necrotic type.[22]

Thallium alters mitochondrial functionality

It is known that changes in extracellular lactate and ethanol concentration levels are generated by changes in the energetic metabolism of the cell.[33, 34] For this reason we analyzed the functionality of mitochondria, considering two key indicators of mitochondrial efficiency: the intra mitochondrial ROS level (mtROS) and the transmembrane potential $\Delta\Psi_m$. All the measures were performed both after 48 h exposure to TlCl and during the recovery in TlCl-free medium (at 24, 48 and 72 h).

The mtROS level was determined using the redox-sensitive fluorescent probe MitoTracker™ Red CM-H_2XROS (MT-ROS) and quantifying its fluorescence in the images acquired at high resolution by confocal microscopy from living neurons (see methods).

After 48 h exposure to TlCl (1, 10 and 100 μg/L) a significant dose-dependent mtROS increase was observed, mainly for TlCl doses ≥ 10ug/L (Figure 2).

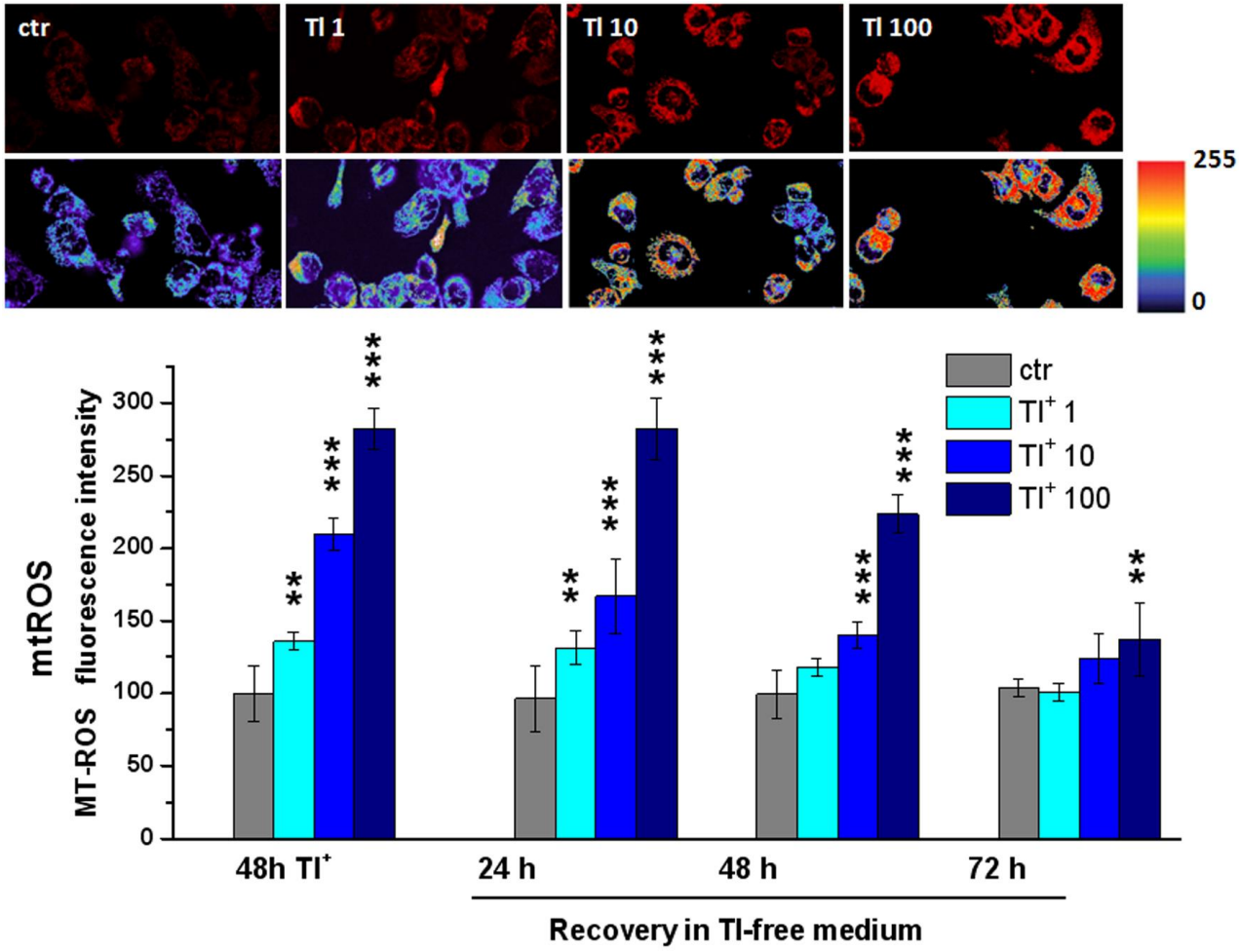

Figure 2. Normalized mtROS level after 48 h exposure to TlCl (1, 10 and 100 μg/L) and during the recovery in TlCl-free medium (at 24, 48 and 72 h). Data were normalized with respect to the control value. The pseudo-colored vertical bar in the neuron images represents the relative fluorescence scale (red indicates highest mtROS values). Asterisks indicate significant differences (Kruskal-Wallis test) with respect to control cultures (* =P <0.05; ** P<0.01; *** = P<0.001; N =3 independent experiments).

The increase of mtROS in the TlCl exposed neurons was significant with respect to controls for 1 μg/L TlCl (P< 0.01) and for 10 and 100 μg/L (P < 0.001), just after 48h exposure and 24 h after the TlCl-containing medium was replaced with TlCl-free medium. The increase of mtROS in the 10 and 100 μg/L TlCl exposed neurons was significant (P < 0.001) with respect to controls also 48 h after the TlCl-containing medium was replaced with TlCl-free medium. The increase of mtROS level with respect to the control remained significant (P < 0.01) 72 h after the TlCl-containing medium was replaced with TlCl-free medium only in 100 μg/L TlCl exposed neurons.

Thus, for the lower TlCl dose (1 μg/L), the recovery process was completed within 72 h, on the contrary, for TlCl ≥ 10 μg/L, mtROS level remained higher even after 72 h. The substantial increase of mtROS observed in cell cultures exposed to 100 μg/L TlCl and the observation of the switch of cell death from apoptotic to necrotic,[22] could suggest the induction of a substantial impairment of the mitochondrial oxidative phosphorylation and a decoupling of the electron transfer chain. These two events are well known to produce a rapid fall of the cellular energy charge. This energy depletion could explain the impossibility of initiating the apoptosis, which is an active process that requires ATP.

Interestingly, + 30% mtROS increase produced by 1 μg/L TlCl did not induce cell death nor an evident substrate detachment in HN9.10e neurons, indicating a fair degree of neuronal resistance to oxidative stress. However, it gave a moderate neurite loss. One hundred and 170% increase of

mtROS produced by 10 and 100 μg/L Tl, respectively, were closely correlated with the dramatic neurite shortening and adhesion loss (Figure 1).

In the same cell cultures we measured the variation of the mitochondrial transmembrane potential ($\Delta\Psi_m$), another sensitive indicator of mitochondrial integrity. Although $\Delta\Psi_m$ can physiologically vary within a wide range, its marked or prolonged decrease is considered the hallmark of energetic dysfunction, often leading to the irreversible commitment to death.

$\Delta\Psi_m$ was assessed by the quantitative analysis of the TMRM fluorescence, detected by confocal microscopy (see methods).

We followed the changes of TMRM fluorescence comparing TlCl-exposed neurons with untreated controls maintained in TlCl-free medium. Figure 3 shows the trend of mitochondrial potential and representative confocal images of control *vs* TlCl-treated neurons after 48 h exposure to TlCl (1, 10 and 100 μg/L) and the recovery in TlCl-free medium (at 24, 48 and 72 h).

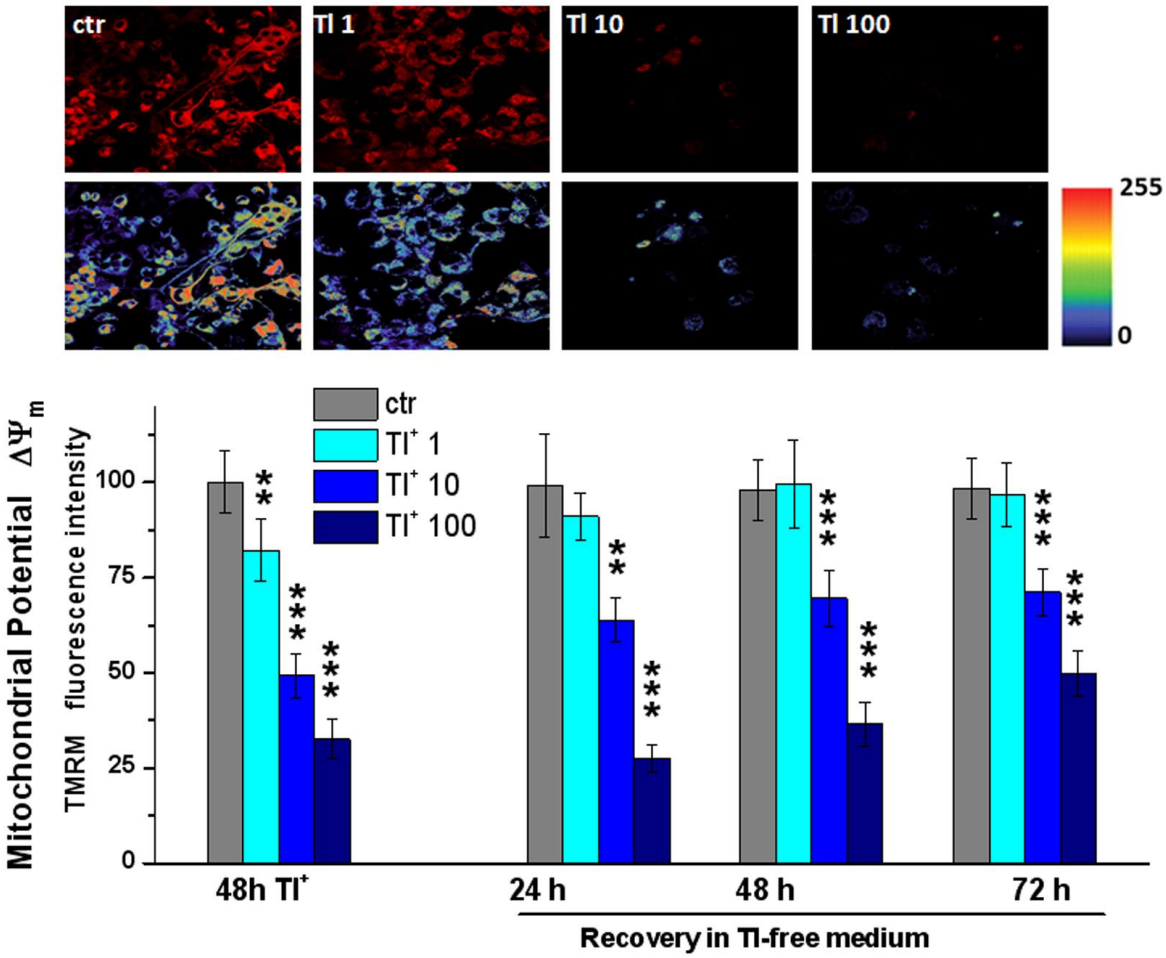

Figure 3. Mitochondrial potential $\Delta\Psi_m$ and representative confocal images of control *vs* TlCl – treated neurons after 48 h exposure to TlCl (1, 10 and 100 µg/L) and during the recovery in TlCl-free medium (at 24, 48 and 72 h). The pseudocolored vertical bar represents the relative fluorescence scale (red indicates highest $\Delta\Psi_m$ values). Asterisks indicate significant differences (Kruskal-Wallis test) with respect to control cultures (* =P <0.05; ** P<0.01; *** = P<0.001; N =3 independent experiments).

TlCl exposures induced a significant decrease of $\Delta\Psi_m$ across the inner membrane, measured as a reduced intensity of the TMRM fluorescence, in a dose-dependent manner (Figure 3).

The decrease of $\Delta\Psi_m$ in the TlCl exposed neurons was significant with respect to controls for 1 µg/L TlCl ($P< 0.01$) and for 10 and 100 µg/L ($P < 0.001$), just after 48 h exposure. $\Delta\Psi_m$ was significantly

recovered in TlCl-free medium 24 h after the exposure only in the case of 1 μg/L TlCl. The recovery in TlCl-free medium of $\Delta\Psi_m$ never occured in the case of the exposure to 10 and 100 μg/L TlCl ($P < 0.01$ or $P < 0.001$ as reported in Figure 3).

This trend was symmetric and comparable with the trend of mtROS variations during exposure and recovery. These data are consistent with a mitochondrial damage, which persists after the TlCl removal, likely because of the accumulation and the prolonged retention of TlCl ions into the mitochondrial matrix.

Thus, the dose-dependent increase of mtROS due to TlCl exposure was significant at all the concentrations investigated and decreased during the recovery in TlCl-free medium for $t \geq 48$ h only for TlCl ≤ 1 μg/L and for $t \geq 72$ h only for TlCl ≤ 10 μg/L. Mitochondrial potential $\Delta\Psi_m$ decreased significantly after 48 h exposure for all the doses investigated and it was never recovered except for 1 μg/L TlCl.

The mitochondrial targeting of TlCl observed in these experiments is particularly relevant in accounting for its neurotoxicity, given the extraordinary sensitivity of nervous tissue to energetic impairment.

The inversion of the ATP synthase masks the initial loss of $\Delta\Psi_m$

Considering that TlCl ions freely permeate both the plasma membrane and the inner mitochondrial membrane through the K^+ channels and that the ion exchanges are extremely rapid, we investigated if the toxic effect of TlCl on HN9.10e neurons was detectable even after shorter exposure times (3 h instead of 48 h). We took into account two parameters: (i) $\Delta\Psi_m$, which is rapidly modified by the mitochondrial stressors, in the absence or presence of oligomycin added in the cell medium 30 min before the end of the experiment; (ii) the free Ca^{2+} level in cytoplasm, commonly considered a sensitive indicator of homeostatic unbalance. Oligomycin is an inhibitor of the enzyme ATP synthase and is able to unmask mitochondria impairment.[36] It is known, indeed, that under stress

conditions the mitochondria, although damaged, may maintain their $\Delta\Psi_m$ by hydrolyzing glycolytic ATP, reversing the enzyme ATP synthase.[36]

In order to reveal whether, in TlCl-treated neurons, this "safety" process was activated, we performed the experiments (controls and TlCl exposed neurons) in the presence of 1 μg/ml oligomycin. This inhibitor suppresses the ATP synthesis and prevents the dissipation of the electrochemical gradient $\Delta\Psi_m$, producing a $\Delta\Psi_m$ increase only in those cells with functional mitochondria, which are actively synthetizing ATP.

The oligomycin test was performed in the last 30 min of the 3 h exposure of HN9.10e neuron cultures to the selected TlCl doses (1, 10 and 100 μg/L) and in the last 30 min of the 24 recovery time in TlCl-free medium in order to explore if, once TlCl was removed from the culture media, mitochondria restored their functionality. The TMRM fluorescence intensity was evaluated in treated *vs* control cultures and the results are shown in Figure 4.

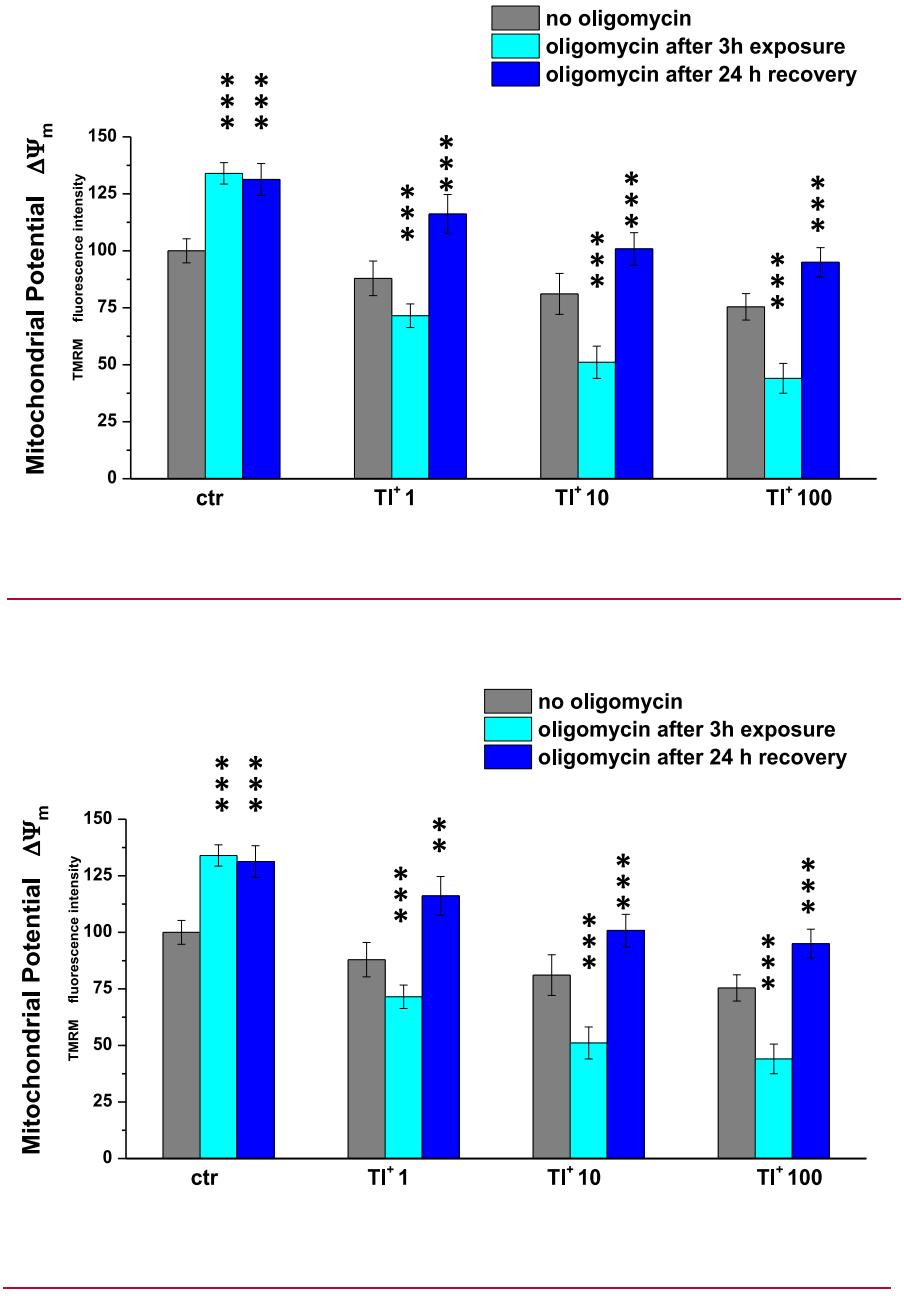

Figure 4. Mitochondrial potential $\Delta\Psi_m$ 3 h after the exposure to TlCl (1, 10 and 100 µg/L) without oligomycin and with oligomycin (1 µg/ml) added in the last 30 min of the 3 h exposure (when TlCl was still present in the medium) and of the 24 h recovery in TlCl-free medium. Asterisks indicate significant differences (Kruskal-Wallis test) with respect to the ~~respective no oligomycin~~oligomycin-treated ~~-~~control cultures (* =P <0.05; ** P<0.01; *** = P<0.001; N =3 independent experiments). The statistical comparison among no oligomycin controls is described in the text.

In the presence of oligomycin 3 h after the exposure to TlCl we observed a dose dependent significant decrease of $\Delta\Psi_m$: with respect to control, not exposed neurons: 12 ± 8% ($P < 0.05$), 19 ±9 ($P < 0.001$) and 25 ± 6% ($p < 0.001$) for cells treated with 1, 10 and 100 μg/L, respectively (N =3 independent experiments).

In control, not exposed neurons the addition in the medium of oligomycin evidenced a physiological, significant increase ($p<0.001$) of $\Delta\Psi_m$, as indicated by the TMRM fluorescence enhancement (about +30%). This demonstrates that, in control conditions, the mitochondrial ATP balance was positive and that the mitochondria were net generators of ATP.

After 3 h exposure to TlCl, oligomycin caused, instead, a dose-dependent, significant ($p<0.001$ for all doses) decrease of $\Delta\Psi_m$ with respect to the neurons not treated with oligomycin, indicating that part of the mitochondria in TlCl-exposed neurons were damaged and that their potential was maintained with energy consumption by the ATP synthase reversal. This result clearly shows that mitochondria were relying on glycolytic ATP hydrolysis, i.e. they degraded more ATP than they produced with a negative mitochondrial ATP balance.

These results are important in order to demonstrate that the relatively moderate decrease of $\Delta\Psi_m$ observed in TlCl-exposed neurons was, actually, partially masked by the ATP synthase reversal. The real magnitude of the $\Delta\Psi_m$ loss after 3 h TlCl treatment was revealed only in presence of oligomycin (Figure 4, cyan bars).

To establish how long the mitochondrial dysfunction persisted, we repeated the oligomycin test on control and TlCl-treated neurons after 24 h recovery in TlCl-free medium (Figure 4, blue bars). The analysis of TMRM fluorescence did not reveal a significant recovery with respect to neurons nor exposed to TlCl neither for TlCl 1 μg/L ($p<0.01$) nor for TlCl $\geq$ 10μg/L ($p<0.001$), i.e. mitochondria did not recover a complete, efficient oxidative phosphorylation, with $\Delta\Psi_m$ comparable with control neurons. Thus, the oligomycin test, besides the ATP synthase reversal during the 3 h TlCl treatment, revealed a persistent residual mitochondrial dysfunction due to 1, 10 and 100 μg/L TlCl treatment even 24 h after recovery in TlCl-free medium.

Thus, the high risk of TlCl exposure was furthermore evidenced by a very short exposure time (3 h) that altered the mitochondrial functionality and by the slow recovery, which suggests a long retention of this ion inside neurons.

TlCl exposure raises the free Ca^{++} level in cytoplasm

Mitochondria play a central role also in buffering and releasing calcium so that a prolonged mitochondrial dysfunction can produce a cytosolic Ca^{2+} overload that contribute to a severe cellular dysfunction and death.[37] In light of these findings, to provide further information on the neuronal damage following a fast, 3 h exposure to TlCl we also measured the changes of the intracellular free Ca^{2+} level by the fluorescent probes Fluo3 acetoxymethyl ester (Fluo-3AM). A significant increase of cytoplasmic Ca^{++} was observed after 3 h exposure to 1, 10, 100 μg/L TlCl (Figure 5, $P < 0.001$).

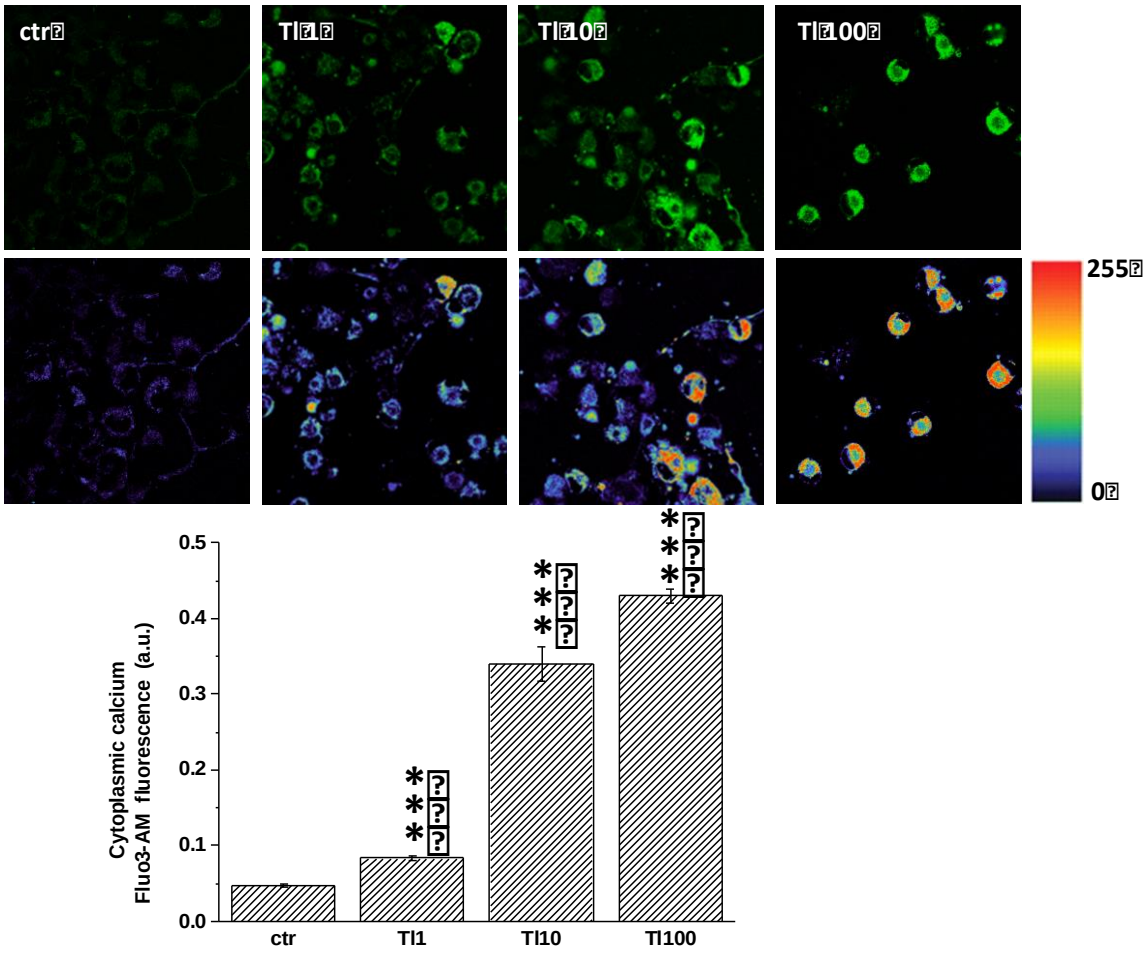

Figure 5. Intracellular free Ca^{2+} level measured by the fluorescent probe Fluo-3 acetoxymethyl ester (Fluo-3AM) in control and TlCl–treated neurons after 3 h exposure to 1, 10 and 100 μg/L TlCl. Asterisks indicate significant differences (Kruskal-Wallis test) with respect to control cultures (* =P <0.05; ** P<0.01; *** = P<0.001; N =3 independent experiments).

Although the experiments with Fluo-3AM probe are not able to provide any information about the sub-cellular source of Ca^{2+}, it is possible to hypothesize that the significant, dose-dependent increase of cytoplasmic Ca^{2+} is compatible with the mitochondrial dysfunction.

In summary, the increase of cytoplasmic calcium as well as the dose-dependent alteration of mitochondrial ROS (mtROS) level and of transmembrane mitochondrial potential ($\Delta\Psi_m$) have been observed also for very low TlCl doses (1 μg/L). The treatment with the ATP synthase inhibitor oligomycin has shown that the mitochondrial function was damaged even more than that evidenced by the simple quantification of the TMRM fluorescence.

Ethanol, a marker of mitochondrial impairment.

The data herein reported suggest that the TlCl-induced impairment of mitochondria may be correlated with the production of EtOH. Figure 6 shows the Pearson correlation plot of EtOH concentration levels in cell culture medium (CCM) (mean value normalized with respect to the concentration values of the controls not exposed to Tl) *vs* the mitochondrial potential value (mean value) in the experiments performed.

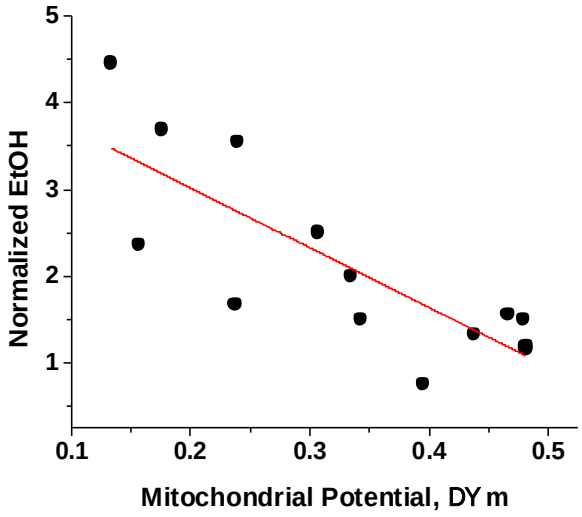

Figure 6. Correlation plot of EtOH concentration levels (mean value normalized with respect to the concentration values of the controls not exposed to Tl) *vs* the mitochondrial potential value (mean value) in the experiments performed. Pearson partial correlation was conducted (r= -0.817, P< 0.01, confidence intervals (99%) = -0.383 - -0.955, N=15).

The results reported above show that TlCl induce a severe dose-dependent, mitochondrial dysfunction, which is quantified by $\Delta\Psi_m$ value. Figure 6 clearly demonstrate that the mitochondrial dysfunction strongly correlates (r^2= 0.667, P< 0.01) with EtOH produced by neurons and determined in the CCM.

EtOH concentration in CCM ranges between 0.3 in neurons exposed to 10 μg/L TlCl and 0.6 mmol/L in neurons exposed to 100 μg/L TlCl, and it was 0.18 mmol/L in nor exposed neurons .

Interestingly, Gray et al. reported that higher EtOH concentrations were found unexpectedly, indeed, in cerebrospinal fluid of ALS patients.[30] that EtOH concentration in cerebrospinal fluid of ALS patients was about 0.079 mmol/L, about 3-4 times higher than in controls (0.026 mmol/L). These concentration values are one order of magnitude lower than those found in CCM, and the comparison of these values (EtOH concentration in CCM and in cerebrospinal fluid) has no biological mean.

However it is interesting to observe that in both cases the impairment of the mitochondrial function increase the EtOH concentration by 2-4 times.

Considering that these concentrations can be easily measured using specific commercial sensors,[38, 39] these results, if confirmed by further studies, suggest that EtOH can be proposed *in vitro* as a marker of mitochondrial functionality and *in vivo* as a marker of disease. The volatile compounds change precociously, indeed, and are excellent biological markers of metabolic defects and pathological conditions.[41, 42]

A further development of this work is also to understand if these anomalous metabolic effects caused by TlCl exposure in nervous cells are induced by any other type of stress agents. Also in this case, the relationship between cellular stress and EtOH production could be of great diagnostic interest.

Conclusions

The 48 h exposure to low doses (1-100 μg/L) of heavy metal Thallium (Tl) has significant effects on morphology and mitochondrial function of living hippocampal HN9.10e neurons.

Mitochondria are the key sub-cellular target of TlCl neurotoxic action whose metabolic effect is the switch of the metabolism from oxidative to the production of lactate (Warburg effect) and EtOH.[22]

These results highlight that Tl doses considered safe by drinking water regulation, for example, (e.g. 1 μg/L, which is below the maximum contaminant level of Tl in drinking water fixed by U.S. EPA at 2 μg/L),[40] are actually able to induce significant and long-lasting changes in the mitochondrial function.

MATERIALS AND METHODS

Chemicals and Reagents

Thallium chloride (224898), DMEM-F12 culture medium, HEPES buffer and oligomycin (O4876) were purchased from Sigma-Aldrich-Fluka (Milan, Italy). Thallium compounds are toxic and should be handled with caution in a ventilated fume hood, using appropriate protective clothing.

The fluorescent probes MitoTracker ™ Red CM-H_2XRos (MT-ROS), tetramethylrhodamine methyl ester (TMRM) and Fluo-3 acetoxymethylester (Fluo-3AM), were purchased from Thermo Fisher Scientific, (Waltham, MA, USA), they were stored as concentrated stock solutions (1 mM) in DMSO and diluted in DMEM-F12 culture medium before use.

Cell culture

The HN9.10e cell line was originally developed by Lee and Wainer by immortalization of murine hippocampal neuroblasts through the somatic cell fusion with N18TG2 neuroblastoma cells.[43] HN9.10e neurons were grown in DMEM-F12 (1:1) medium HEPES buffered, supplemented with 2 mM L-glutamine, 50 UI/mL penicillin and 50 mg/mL streptomycin, at 37 °C in humidified atmosphere containing 5% CO_2. Neurons, seeded at 20,000 cell/cm^2 in culture flasks containing 5 mL of medium, or on glass coverslips for confocal microscopy experiments, were left in culture for 4 days before treatments in order to allow substrate adhesion and growth to an optimal 40-60% confluence. HN9.10e neurons were treated for 3 or 48h with TlCl 1, 10 or 100 µg/L. After incubation, they were washed twice with complete culture medium. All treatments have been repeated in at least 3 independent experiments.

Neurite length measurement

The neurite tracing algorithm (Automated Neurite Outgrowth Module) of the MetaMorph 5.0 software (Universal Imaging Corporation, West Chester, PA) was used to quantify the neurite length of control and TlCl-treated neurons. Briefly, the transmitted light images (1024x1024 pixel resolution) of HN9.10e neurons, grown in monolayer, were initially processed with the MetaMorph software for thresholding. Images were de-noised using a Gaussian filter, then cell bodies and neurites

were automatically distinguished by the neurite-tracing algorithm. Each neurite was assigned to the appropriate cell body and all neurites of each image were approximated with a segmented line (skeletonized profile). The length of each neurite was calculated as the sum of all the skeletonized neurite segments. For each experimental group not less than 450 images were randomly selected from N =3 independent experiments, for a total of at least 2500 neurons examined for each treatment.

Confocal imaging in living neurons

For single cell imaging, HN9.10e neurons were grown on glass coverslips (13-mm diameter) in 24-well plates and then transferred to a thermostatic imaging chamber, maintained at 37 °C, placed on the microscope stage. High resolution (1024 x 1024 pixel) fluorescence images were acquired using a confocal Leica TCS-NT scanning microscope (Leica Microsystems, Mannheim, Germany) equipped with a HeNe/Ar laser source. The appropriate wavelength for excitation each fluorescent probe was selected: λ_{ex}= 488 nm for Fluo-3AM, λ_{ex}= 543 nm for TMRM and MitoTracker™ Red CM-H_2XRos.

Laser power was kept at 15% of maximal power to avoid both photo-damage of cells and photo-bleaching of fluorescent probes. Images were acquired at 1024 × 1024 pixels resolution using Leica Plan Apo oil immersion objectives 40x/1.2 numerical aperture (NA) or 63x/1.4 (NA) and averaged 4 times to improve the signal/noise ratio. For each field both fluorescent and transmitted light images were acquired on separate photomultipliers and eventually merged in offline analysis.

In all experiments at least 2.000 neurons for each experimental group were considered, sampling at least 5 independent fields (400 x 400 μm) in 3 independent experiments. Quantification of fluorescence signals was performed offline, after the subtraction of the background fluorescence, using both MetaMorph 5.0 and MATLAB (The MathWorks, Massachusetts, U.S.A.) analysis software. The auto-fluorescence of non-loaded neurons was negligible compared to the signal recorded from dye-loaded neurons and it was therefore ignored.

Reactive oxygen species measurement

To measure ROS generation in mitochondria, HN9.10e neurons were loaded for 30 min at 37°C with 2 nM MitoTracker™ Red CM-H_2XROS (MT-ROS), then they were washed twice with DMEM-F12 medium. The reduced, non-fluorescent form of this probe accumulates in mitochondria where it is oxidized in proportion to the respiration rate, becoming fluorescent and detectable by confocal microscopy. MT-ROS was excited using λ_{ex}= 543 nm and the emitted fluorescent light was collected through a 590 $\pm$ 10 nm long-pass filter. MT-ROS signal was measured maintaining constant the laser power and photomultiplier sensitivity to allow comparison of fluorescence intensity between control and treated cells. The changes of MT-ROS fluorescence following treatments were normalized to the value of the control experiment. Results were expressed as relative fluorescence intensity F/F0 × 100%, where F is the fluorescence after treatment and F0 is the control fluorescence. The measurements are expressed as average value ± SD.

Mitochondrial membrane potential measurement

Mitochondrial membrane potential was determined by tetramethylrhodamine methyl ester (TMRM), a fluorescent cation that distributes into the mitochondrial matrix of active mitochondria following the electrochemical gradient. TMRM was excited with the 543 nm laser line and emission was collected at 600 $\pm$ 10 nm. HN9.10e neurons were loaded for 30 min at 37°C with 5 nM TMRM, then they were washed twice with DMEM-F12 medium. TMRM fluorescence was measured maintaining constant the laser power and photomultiplier sensitivity in control and treated experimental groups. Results were expressed as relative fluorescence intensity F/F0 × 100%, where F is the fluorescence after treatment and F0 is the control fluorescence.

Analysis of cytosolic Ca^{2+} level

Ca^{2+} imaging experiments were performed loading HN9.10e cells with the Ca^{2+} indicator Fluo-3 acetoxymethylester (Fluo-3AM), that exhibits a fluorescence intensity increase upon Ca^{2+} binding.

Cultures were incubated for 30 min at 37 ◦C in 1 μM Fluo-3AM, followed by two washes with fresh medium, to remove any dye non-specifically associated with cell surface. Then cultures were incubated for a further 30 minutes before imaging to allow a complete de-esterification of the intracellular Fluo-3AM. Measures of Fluo-3AM fluorescence were carried out in a thermostatic imaging chamber at 37°C using the λ_{ex} 488 nm of the HeNe/Ar laser source. Confocal images, acquired by scanning at 1024x1024 pixel resolution, were analyzed offline using both the image analysis software MetaMorph 5.0 (Universal Imaging, West Chester, PA) and MATLAB routines dedicated to fluorescence quantification and background fluorescence subtraction. The intensity of Fluo-3 AM signal was expressed as arbitrary units (A.U.). All measurements were performed in at least 3 independent experiments for each dose, N =5 sampling fields (400 x 400 μm) in each experiment (in total 15 fields from N= 3 independent experiments). In the control conditions, each field contained on average 150 cells.

EtOH analysis by SPME-HS-GC-MS

EtOH was analyzed by SPME sampling of headspace (HS) in GCMS. An Agilent 6850 gas chromatograph, equipped with a split/splitless injector, was used in combination with an Agilent 5975c mass spectrometer. A CTC CombiPAL autosampler was employed for the SPME HS sampling. The vials were incubated at 50°C for 10 min. The SPME fiber was esposed for 5 minutes in the HS and injected in splitless mode into the gas chromatograph. The fiber was flushed inside the injector with helium at 300 mL/min for 15 minutes for cleaning (no carry-over problems were encountered). The inlet liner (1 mm internal diameter) was held at 280°C and the injection was performed in splitless mode (15 s splitless time) in the column (helium flow rate 1 mL/min). Compounds were then separated on a high polarity column (DB-FFAP ; 60 m length; : 60 m; terephtalic acid modified carbowax stationary phase; 0.25 mm inner diameter; 0.5 μm coating) using the following temperature program: 10 min held at 30 °C, 4 °C/min up to 240 °C held for 15 min (55 min total runtime). The temperature of the transfer line was set at 240 °C. After GC separation, EtOH

was ionized in positive EI. The MS acquisition was performed in total ion chromatography (TIC) and in selected ion monitoring (SIM) modes. TIC allowed us the identification of the EtOH, whereas SIM was implemented for quantitative purposes by monitoring m/z of 45, 46 and 31 (100 ms dwell time).

For the calibration of the instrumental response, 5 mL of 0, 0.023, 0.046, 0.23, 0.46 and 2.3 mM EtOH (primary standard solution) were introduced in 10 mL headspace vials (Agilent Technologies, Part No. 8010-0038). For EtOH determination the dynamic linear range (DLR) was 0.002 – 2.5 mM, 0.002 mM LOD, slope 4.65 ± 0.07 (au mM^{-1}), R^2=0.9999. The coefficient of variation (CV%) of measurements performed on the same vial is <2%; the coefficient of variation (CV%) of measurements performed on different vials is < 3 %.

Statistical Analysis.

All data were expressed as means ± S.D. Statistical analysis was performed using OriginPro 7.5 scientific graphing and data analysis software (OriginLab Corporation, MA, USA). Comparisons among multiple groups were assessed using the (XLstat, Microsoft Excel®). Statistical significance was established at $p<0.05$. Statistical significance was determined by using non parametric Kruskal-Wallis test (* =P <0.05; ** P<0.01; *** = P<0.001). A P value <0.05 was considered to be statistically significant. Pearson partial correlation was used for correlation analysis.

Author Information

Corresponding Author

*To whom correspondence may be addressed. E-mail: laura.colombaioni@in.cnr.it; Phone: 0039-050-315-3214. Fax: +39-050-315-3220

Author Contributions

All authors contributed toward design of the research, in interpretation of results, and in writing the paper. Laura Colombaioni performed confocal microscopy. Massimo Onor prepared the samples and Emilia Bramanti performed statistical analysis and conventional chemical analyses.

Funding Sources

This research did not receive any specific grant from funding agencies in the public, commercial, or not-for-profit sectors.

REFERENCES

1. Woods, J. S., and Fowler, B. A. (1986) Alteration of hepatocellular structure and function by thallium chloride: ultrastructural, morphometric, and biochemical studies, *Toxicol Appl Pharmacol 83*, 218-229.

2. Mulkey, J. P., and Oehme, F. W. (1993) A review of thallium toxicity, *Veterinary and human toxicology 35*, 445-453.

3. Goel, A., and Aggarwal, P. (2007) Pesticide poisoning, *The National medical journal of India 20*, 182-191.

4. Méndez-Armenta, M., Nava-Ruiz, C., Fernández-Valverde, F., Sánchez-García, A., and Rios, C. (2011) Histochemical changes in muscle of rats exposed subchronically to low doses of heavy metals, *Environmental Toxicology and Pharmacology 32*, 107-112.

5. Eskandari, M. R., Mashayekhi, V., Aslani, M., and Hosseini, M. J. (2015) Toxicity of Thallium on Isolated Rat Liver Mitochondria: The Role of Oxidative Stress and MPT Pore Opening, *Environmental Toxicology 30*, 232-241.

6. Cerrato, L., Valeri, A., Bueren, J. A., and Albella, B. (2009) In vitro sensitivity of granulo-monocytic progenitors as a new toxicological cell system and endpoint in the ACuteTox Project, *Toxicology and Applied Pharmacology 238*, 111-119.

7. Hanzel, C. E., and Verstraeten, S. V. (2006) Thallium induces hydrogen peroxide generation by impairing mitochondrial function, *Toxicology and Applied Pharmacology 216*, 485-492.

8. Hanzel, C. E., and Verstraeten, S. V. (2009) Tl(I) and Tl(III) activate both mitochondrial and extrinsic pathways of apoptosis in rat pheochromocytoma (PC12) cells, *Toxicology and Applied Pharmacology 236*, 59-70.

9. Gregotti, C., Di Nucci, A., Costa, L. G., Manzo, L., Scelsi, R., Bertè, F., and Faustman, E. M. (1992) Effects of thallium on primary cultures of testicular cells, *Journal of Toxicology and Environmental Health 36*, 59-69.

10. Campanella, B., Onor, M., D'Ulivo, A., Giannecchini, R., D'Orazio, M., Petrini, R., and Bramanti, E. (2016) Human exposure to thallium through tap water: A study from Valdicastello Carducci and Pietrasanta (northern Tuscany, Italy), *Science of the Total Environment 548-549*, 33-42.

11. Campanella, B., Casiot, C., Onor, M., Perotti, M., Petrini, R., and Bramanti, E. (2017) Thallium release from acid mine drainages: Speciation in river and tap water from Valdicastello mining district (northwest Tuscany), *Talanta 171*, 255-261.

12. Galvan-Arzate, S., Martinez, A., Medina, E., Santamaria, A., and Rios, C. (2000) Subchronic administration of sublethal doses of thallium to rats: effects on distribution and lipid peroxidation in brain regions, *Toxicology Letters 116*, 37-43.

13. Davis, L. E., Standefer, J. C., Kornfeld, M., Abercrombie, D. M., and Butler, C. (1981) Acute thallium poisoning: toxicological and morphological studies of the nervous system, *Annals of neurology 10*, 38-44.

14. Nordentoft, T., Andersen, E. B., and Mogensen, P. H. (1998) Initial sensorimotor and delayed autonomic neuropathy in acute thallium poisoning, *Neurotoxicology 19*, 421-426.

15. Slizofski Walter, J., Krishna, L., Katsetos Christos, D., Black, P., Miyamoto, C., Brown Steven, J., Vender, J., Chevres, A., Khan Angabeen, S., McEwan, J., and Dadparvar, S. (1994) Thallium imaging for brain tumors with results measured by a semiquantitative index and correlated with histopathology, *Cancer 74*, 3190-3197.

16. Kim, K. T., Black, K. L., Marciano, D., Mazziotta, J. C., Guze, B. H., Grafton, S., Hawkins, R. A., and Becker, D. P. (1990) Thallium-201 SPECT imaging of brain tumors: methods and results, *Journal of nuclear medicine : official publication, Society of Nuclear Medicine 31*, 965-969.

17. Sugo, N., Yokota, K., Kondo, K., Harada, N., Aoki, Y., Miyazaki, C., Nemoto, M., Kano, T., Ohishi, H., and Seiki, Y. (2006) Early dynamic 201Tl SPECT in the evaluation of brain tumours, *Nuclear Medicine Communications 27*.

18. Holman, B. L., Zimmerman, R. E., Johnson, K. A., Carvalho, P. A., Schwartz, R. B., Loeffler, J. S., Alexander, E., Pelizzari, C. A., and Chen, G. T. (1991) Computer-assisted superimposition of magnetic resonance and high-resolution technetium-99m-HMPAO and thallium-201 SPECT images of the brain, *Journal of nuclear medicine : official publication, Society of Nuclear Medicine 32*, 1478-1484.

19. Bodenheimer, M. M., Banka, V. S., and Helfant, R. H. (1980) Nuclear cardiology. II. The role of myocardial perfusion imaging using thallium-201 in diagnosis of coronary heart disease, *The American Journal of Cardiology 45*, 674-684.

20. Ishihara, M., Taniguchi, Y., Onoguchi, M., and Shibutani, T. (2018) Optimal thallium-201 dose in cadmium-zinc-telluride SPECT myocardial perfusion imaging, *Journal of Nuclear Cardiology 25*, 947-954.

21. LLC, M. N. M. (2016) Thallous Chloride Tl 201 Injection, Diagnostic—For Intravenous Use Initial U.S. approval: 1979, *A120I0 R07/2016*.

22. Colombaioni, L., Onor, M., Benedetti, E., and Bramanti, E. (2017) Thallium stimulates ethanol production in immortalized hippocampal neurons, *PLOS ONE 12*, e0188351.

23. Diaz-Ruiz, R., Rigoulet, M., and Devin, A. (2011) The Warburg and Crabtree effects: On the origin of cancer cell energy metabolism and of yeast glucose repression, *Biochimica et Biophysica Acta (BBA) - Bioenergetics 1807*, 568-576.

24. Ferreira, L. M. R. (2010) Cancer metabolism: The Warburg effect today, *Experimental and Molecular Pathology 89*, 372-380.

25. Gogvadze, V., Zhivotovsky, B., and Orrenius, S. (2010) The Warburg effect and mitochondrial stability in cancer cells, *Molecular Aspects of Medicine 31*, 60-74.

26. Warburg, O. (1956) On the Origin of Cancer Cells, *Science 123*, 309.

27. McManus, I. R., Contag, A. O., and Olson, R. E. (1960) Characterization of Endogenous Ethanol in the Mammal, *Science 131*, 102-103.

28. Dorokhov, Y. L., Shindyapina, A. V., Sheshukova, E. V., and Komarova, T. V. (2015) Metabolic methanol: molecular pathways and physiological roles, *Physiol Rev 95*, 603-644.

29. Garcia-Manteiga, J. M., Mari, S., Godejohann, M., Spraul, M., Napoli, C., Cenci, S., Musco, G., and Sitia, R. (2011) Metabolomics of B to Plasma Cell Differentiation, *Journal of Proteome Research 10*, 4165-4176.

30. Gray, E., Larkin, J. R., Claridge, T. D. W., Talbot, K., Sibson, N. R., and Turner, M. R. (2015) The longitudinal cerebrospinal fluid metabolomic profile of amyotrophic lateral sclerosis, *Amyotrophic Lateral Sclerosis and Frontotemporal Degeneration 16*, 456-463.

31. Komarova, T. V., Petrunia, I. V., Shindyapina, A. V., Silachev, D. N., Sheshukova, E. V., Kiryanov, G. I., and Dorokhov, Y. L. (2014) Endogenous Methanol Regulates Mammalian Gene Activity, *PLOS ONE 9*, e90239.

32. Meshitsuka, S., Morio, Y., Nagashima, H., and Teshima, R. (2001) 1H-NMR studies of cerebrospinal fluid: endogenous ethanol in patients with cervical myelopathy, *Clinica Chimica Acta 312*, 25-30.

33. Mazat, J. P., Ransac, S., Heiske, M., Devin, A., and Rigoulet, M. (2013) Mitochondrial energetic metabolism-some general principles, *IUBMB life 65*, 171-179.

34. Melser, S., Lavie, J., and Bénard, G. (2015) Mitochondrial degradation and energy metabolism, *Biochimica et Biophysica Acta (BBA) - Molecular Cell Research 1853*, 2812-2821.

35. Hurtley, S. M. (2016) Apoptosis, necrosis, and pyroptosis, *Science 352*, 48.

36. Brand, Martin D., and Nicholls, David G. (2011) Assessing mitochondrial dysfunction in cells, *Biochemical Journal 435*, 297.

37. Williams, G. S., Boyman, L., Chikando, A. C., Khairallah, R. J., and Lederer, W. J. (2013) Mitochondrial calcium uptake, *Proc Natl Acad Sci U S A 110*, 10479-10486.

38. Samphao, A., Butmee, P., Saejueng, P., Pukahuta, C., Svorc, L., and Kalcher, K. (2018) Monitoring of glucose and ethanol during wine fermentation by bienzymatic biosensor, *Journal of Electroanalytical Chemistry 816*, 179-188.

39. Liu, J., Wang, T., Wang, B., Sun, P., Yang, Q., Liang, X., Song, H., and Lu, G. (2017) Highly sensitive and low detection limit of ethanol gas sensor based on hollow ZnO/SnO2 spheres composite material, *Sensors and Actuators B: Chemical 245*, 551-559.

40. United States Environmental Protection Agency. (2009) TOXICOLOGICAL REVIEW OF THALLIUM AND COMPOUNDS (CAS No. 7440-28-0), EPA/635/R-08/001F, http://www.epa.gov/iris.

41. Hakim, M., Broza, Y. Y., Barash, O., Peled, N., Phillips, M., Amann, A., and Haick, H. (2012) Volatile Organic Compounds of Lung Cancer and Possible Biochemical Pathways, *Chemical Reviews 112*, 5949-5966.

42. Shirasu, M., and Touhara, K. (2011) The scent of disease: volatile organic compounds of the human body related to disease and disorder, *Journal of biochemistry 150*, 257-266.

43. Lee, H. J., Hammond, D. N., Large, T. H., Roback, J. D., Sim, J. A., Brown, D. A., Otten, U. H., and Wainer, B. H. (1990) Neuronal properties and trophic activities of immortalized hippocampal cells from embryonic and young adult mice, *The Journal of neuroscience : the official journal of the Society for Neuroscience 10*, 1779-1787.